EARTHQUAKE ENGINEERING AND STRUCTURAL DYNAMICS
Earthquake Engng. Struct. Dyn. **28**, 1143–1162 (1999)

EXPERIMENTAL STUDY ON THE ASEISMIC CAPACITY OF A WOODEN HOUSE USING SHAKING TABLE

JEONG-MOON SEO[1,*], IN-KIL CHOI[1] AND JONG-RIM LEE[2]

[1]*Integrated Safety Assessment Team, Korea Atomic Energy Research Institute, P.O. Box 105, Yusong, Taejon 305-600, Korea*
[2]*Korea Electric Power Research Institute, Korea*

SUMMARY

The aseismic capacity of a typical Korean wooden house built using traditional construction methods is quantitatively estimated. Tenon joints were used in wooden frames. Two 1 : 4 scale models were tested for rock and soil foundation conditions. Scaled real earthquake time histories were input for the tests. The natural frequency and modal damping ratio of the wooden house in the elastic range were 1·66 Hz and 7 per cent, respectively. The Peak Ground Acceleration (PGA) at the collapse of the house at the soil site was 0·25g, whereas PGA for moderate damage at the rock site was 0·6g. A significant reduction in acceleration response and increase in displacement response was observed for rock and soil foundation conditions, respectively. The wooden house studied is much more vulnerable at soil sites than at rock sites due to the rich low-frequency contents of the input motion and the flexible characteristics of the wooden house. Non-linear dynamic analyses using the modified Double-Target model were compared with test results. The modified Double-Target model appropriately simulates the non-linear inelastic behaviour of a wooden house with tenon joints. Copyright © 1999 John Wiley & Sons, Ltd.

KEY WORDS: buildings; wooden house; earthquakes; aseismic capacity; shaking table test

1. INTRODUCTION

The number of historical earthquakes in Korea between 2 AD and 1905 is about 1900. Among the historical earthquake records, approximately 15 events include descriptions of house collapses followed by loss of lives. Six of these events occurred at a typical soft soil site, in the Kyungju City area, with about 20 m thick sand-gravel deposits. The locations of the damaged areas for the rest of the events are scattered widely, where the foundations are generally regarded as hard rock condition with thin soft soil layers. The estimated intensities of historical earthquake records of house collapses vary from MM intensity V to X according to the experts' opinions. The Peak Ground Acceleration (PGA) of MMI V ranges from 0·014g to 0·044g and that of MMI X varies

* Correspondence to: Jeong-Moon Seo, Integrated Safety Assessment Team, Korea Atomic Energy Research Institute, P.O. Box 105, Yusong, Taejon 305-600, Korea.

Received 25 November 1998
Revised 23 March 1999
Accepted 26 April 1999

CCC 0098–8847/99/101143–20$17·50

from 0·562g to 2·754g, according to the empirical relationship[1] between intensity and peak ground acceleration. This large variability of ground acceleration makes it difficult to estimate the maximum PGA level of historical earthquakes.

A series of tests were performed to provide some quantitative basis for the estimation of the maximum PGA level in seismic hazard analysis in areas of Korea with low (or moderate) seismicity. Structural details of the traditional wooden house such as dimension, joint type, etc., and the load carrying characteristics of wooden frames were identified.[2–4] The unique features of the traditional wooden house may reveal structural behaviours differing from those of other countries during earthquakes, and the direct use of the MM intensity scale may add some additional uncertainty.

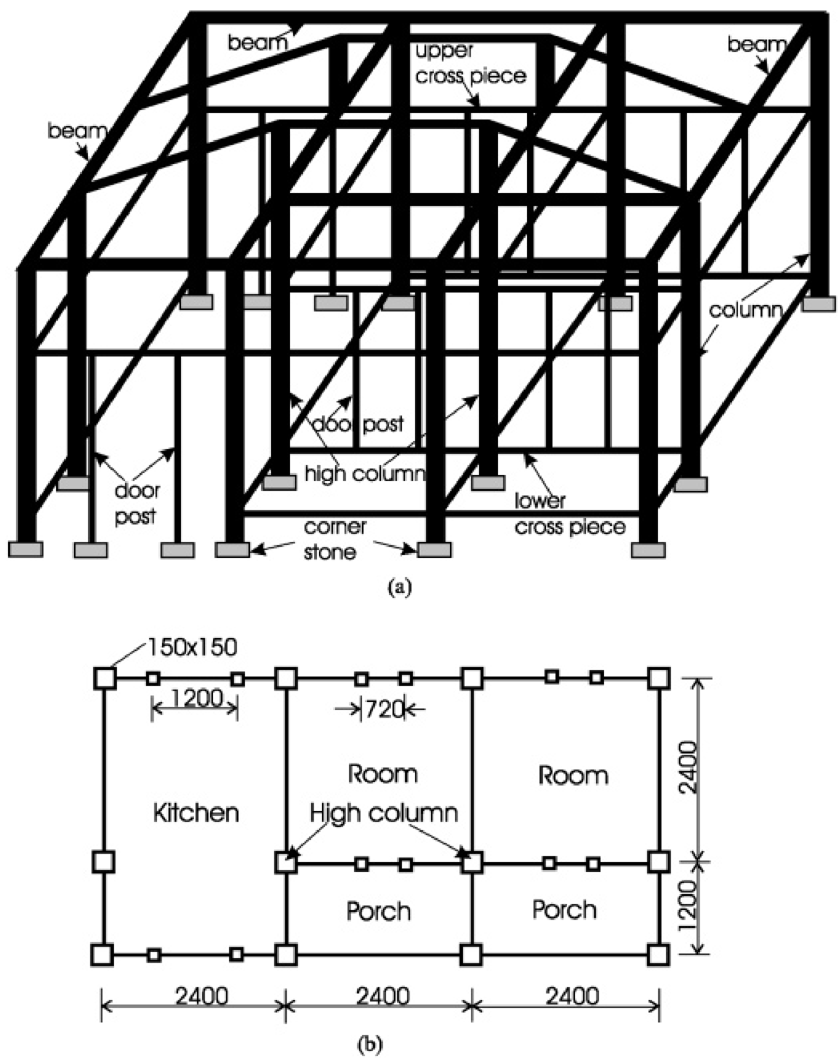

Fig. 1. Structure of the prototype wooden house (unit: mm); (a) perspective view, (b) plan view

In this paper, the results of shaking table tests of 1 : 4 scale models of the ancient commoner's wooden house with tenon joints are described. Two models were fabricated from fresh pine lumber that was typically used in the past. Typical earthquake motions recorded in rock and soil sites were input to the test. The PGA level was increased step by step until the model experienced severe damage or failure. The results of nonlinear dynamic analyses based on the modified Double-Target model[2] were compared with the test results to verify the model.

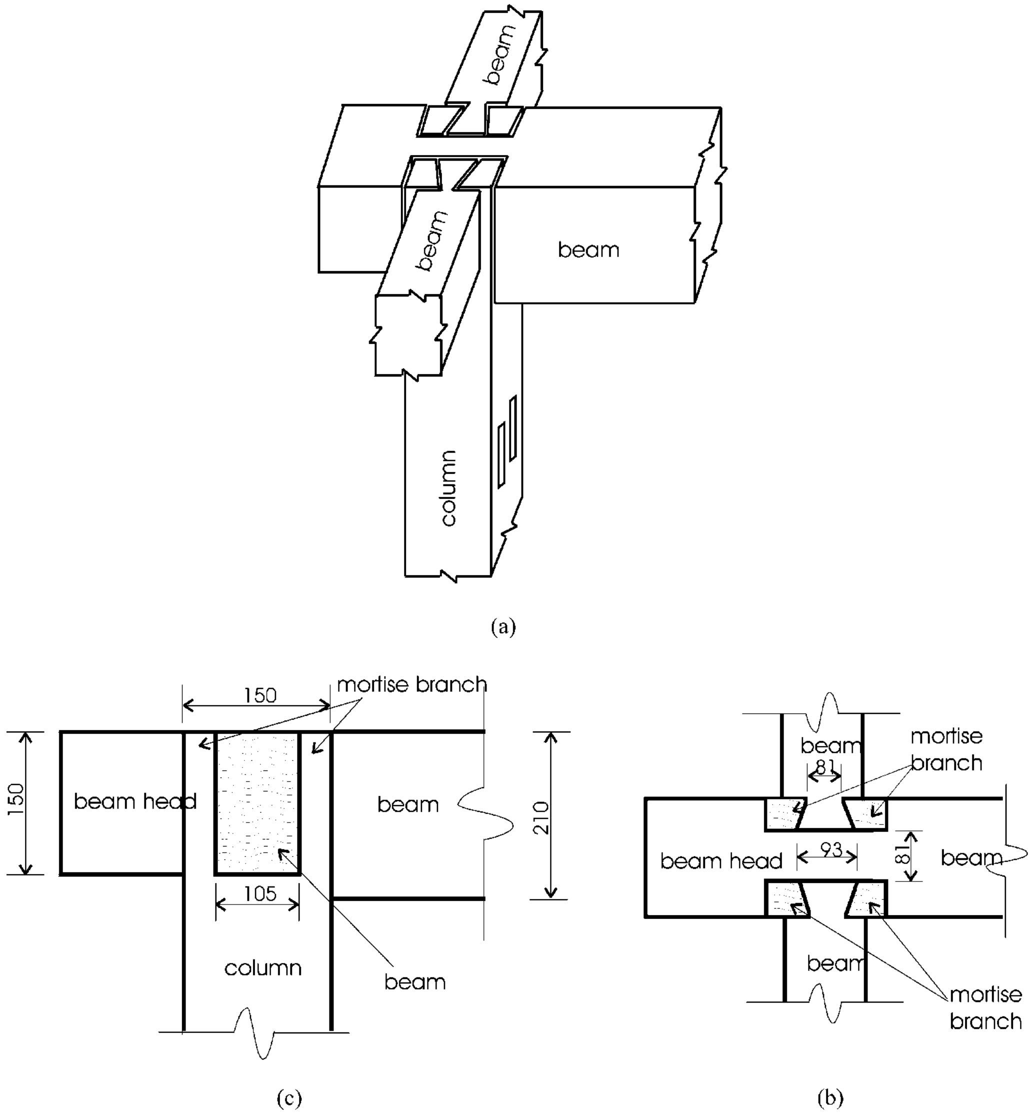

Fig. 2. Details of tenon joint at the top of the column (unit: mm); (a) perspective view, (b) side view; (c) plan view

2. CHARACTERISTICS OF THE PROTOTYPE WOODEN HOUSE AND SCALED MODEL

The size and the materials found in ancient wooden houses differed depending on social stratum and the geographical region in Korea. The most common type of residential house in the ancient period up to the 19th century was a three-bay-straw-roof wooden house consisting one kitchen, two rooms and a porch as shown in Figure 1. Tenant farmers the majority of the ancient agricultural society, lived in such house. This was chosen as a prototype house in this study.

The dimension of the prototype house is $7{\cdot}2$ m (long) $\times$ $3{\cdot}6$ m (wide) $\times$ 2.9 m (high). Two types of wooden frame,[2] type 1 for connecting the perimeter columns and type 2 for connecting an inner high-column and two perimeter columns in the transverse direction, were used. The beam-column joint typically used at the top of the column is a tenon (Figure 2), and the joint between cross member and column is a dovetail. The end of each member is cut in shape and assembled together to form a joint. Nail or bolt is not used. Pine lumber is used for structural members. The trunks of either kaoliang or bush clover plastered with mud form the partition walls in the frame. Rafters with a diameter 90 mm are placed at 300 mm intervals at the roof. Mud plaster of 50–70 mm thick and straw thatches of 300–450 mm thick are overlain on the rafters. The weight of the roof is about 170 kg/m^2. Natural stones two or three times bigger than the column size having a relatively flat surface are used as cornerstones. The bottom face of the column is trimmed to contact tightly at the surface of the cornerstone and the structure freely stands on it (Figure 3).

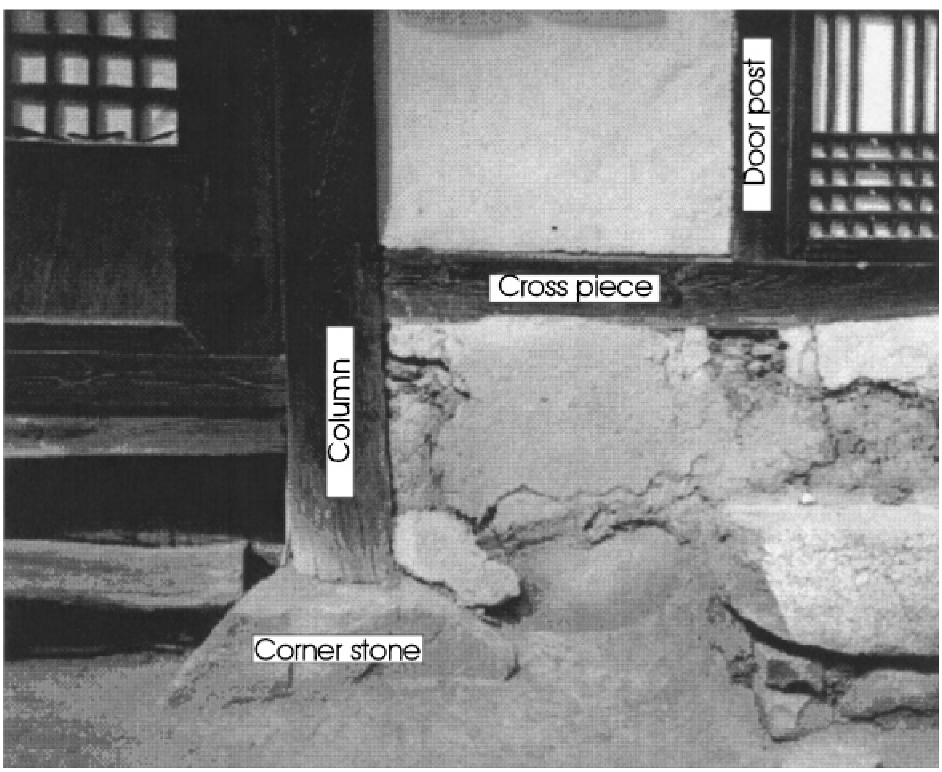

Fig. 3. Typical connection between column and cornerstone

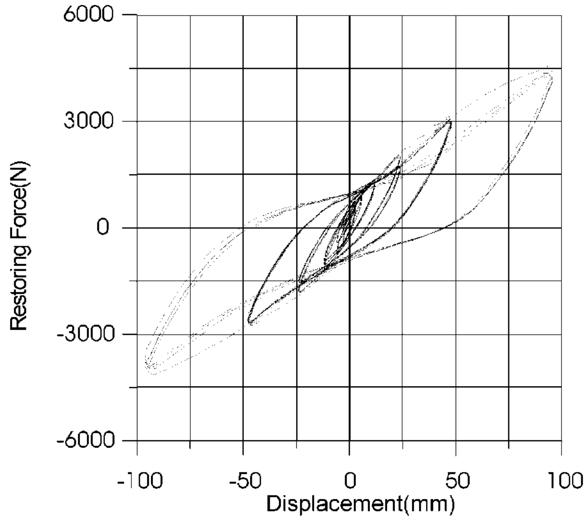

Fig. 4. Hysteretic load–displacement curve of the Type 2 frame

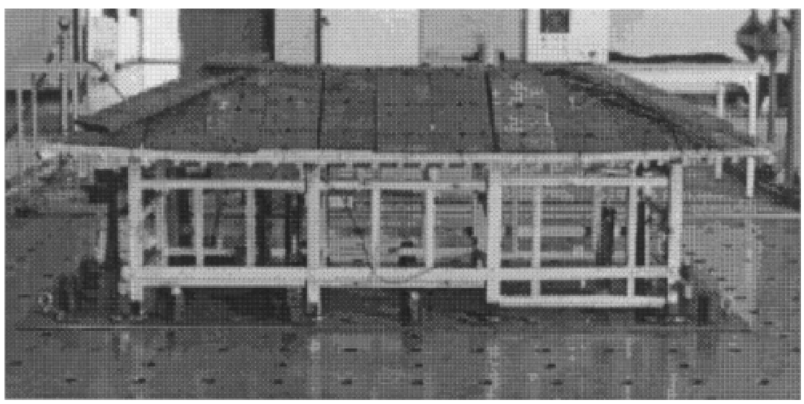

Fig. 5. Overview of a model assembled for test

The lateral load capacity and the skeleton curves under cyclic load of each frame type were obtained from the tests on full-scale models.[2–4] Figure 4 shows a typical example of hysteretic curves for the type 2 frame. It is noted that the curves show large non-linearity and inelasticity.

Two 1 : 4 scale models which were nominally identical were fabricated with fresh pine lumber.[5,6] Two different carpenters with comparable skill made each model. The beam-column joints of the frames were also scaled. The artificial mass method was applied in the model test. The mass of the roof, one half of the wall masses, and added masses were lumped at the roof level. A total mass of 930 kg made of 150 mm (wide) × 600 mm (long) × 25 mm (thick) steel plates was uniformly distributed at the roof, as shown in Figure 5. Both ends of the rafters in the roof frame were nailed to the beams to place steel plates without increasing the stiffness of the model. Steel plates were fastened to the rafters by thin wires.

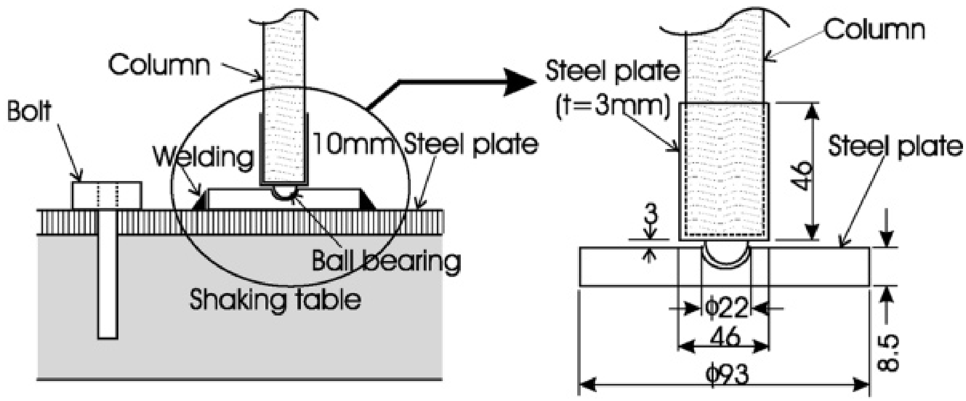

Fig. 6. Detailed view of column-cornerstone connection used in model tests (unit: mm)

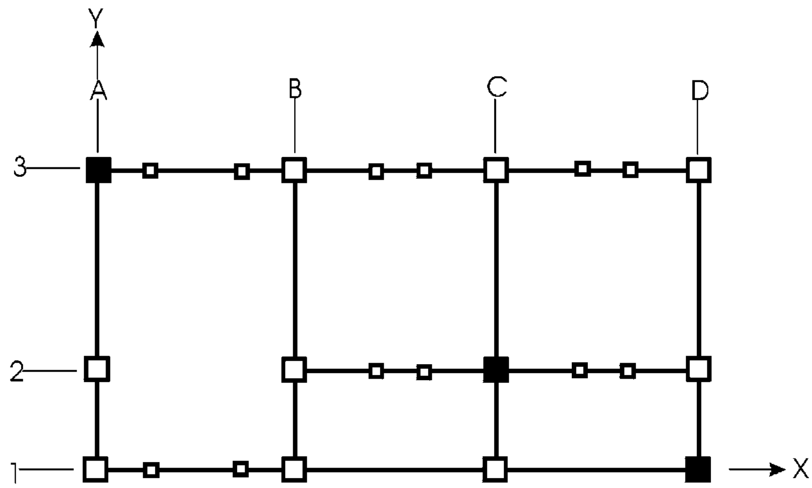

Location	LVDT	Accelerometer
A-3 Top	x,y	x,y,z
C-2 Top	x,y	x,y,z
D-1 Top	x,y	x,y,z

Fig. 7. Location and type of sensors for tests

The boundary condition between the cornerstone and the bottom of the column was assumed to be a hinge and was modelled by mechanical devices specially made of ball bearing as shown in Figure 6. The assumption of the hinge boundary is based on the facts that the contact surface is irregular in plane and the mass centre is located at the top of the flexible frame. Because of this, rotation at the contact surface rather than sliding is more likely to happen during an earthquake. The scaled model was placed on a 10 mm thick steel plate that was tightly fastened to the shaking table.

3. TESTS OF SCALED MODELS

The size of the shaking table is 4 m × 4 m with 6 degrees of excitation freedom. The capacity of the table is limited by a maximum specimen weight of 30,000 kg, maximum acceleration of $1{\cdot}5g$ and $1{\cdot}0g$ in horizontal and vertical direction, respectively. The maximum frequency of the table is 50 Hz. The table is controlled by an electro-hydraulic servo system.

Nine accelerometers and six Linear Variable Displacement Transformers (LVDT) with 25 mm capacity were installed to measure the responses at the top of the two corner columns and one centre column, as shown in Figure 7. Due to the space limitation of the model in installing sensors, the exact location was slightly modified. Special hinge devices were fabricated and

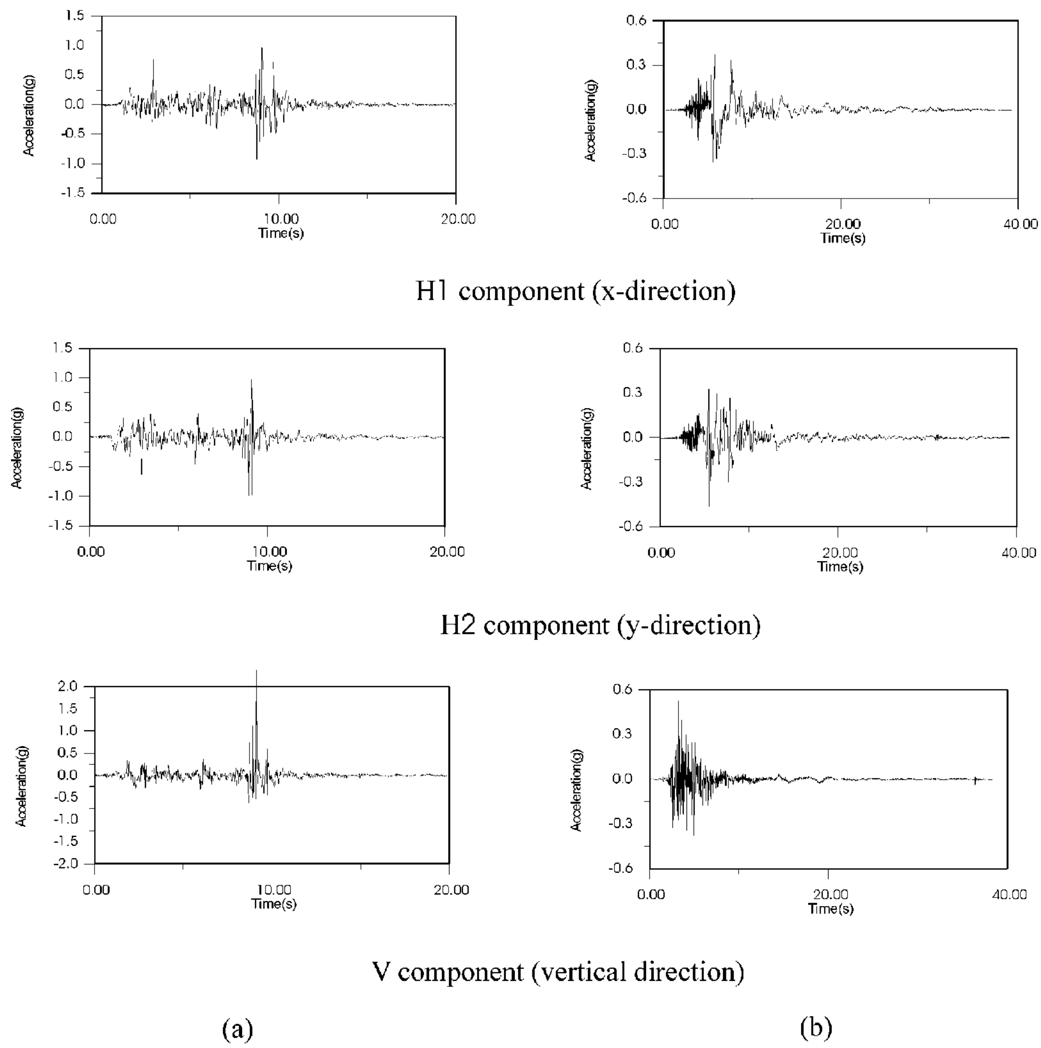

Fig. 8. Time histories for test; (a) Nahanni earthquake (1985), (b) Imperial Valley earthquake (1979)

connected between the column and the LVDT sensor to consider the torsional effect on horizontal displacements.

The Nahanni earthquake, which occurred in eastern Canada in December 1985 and was recorded at a rock site, was input to model 1 as a typical rock motion. The Imperial Valley earthquake of October 1979 in the western United States, recorded at El Centro Array No. 5, was

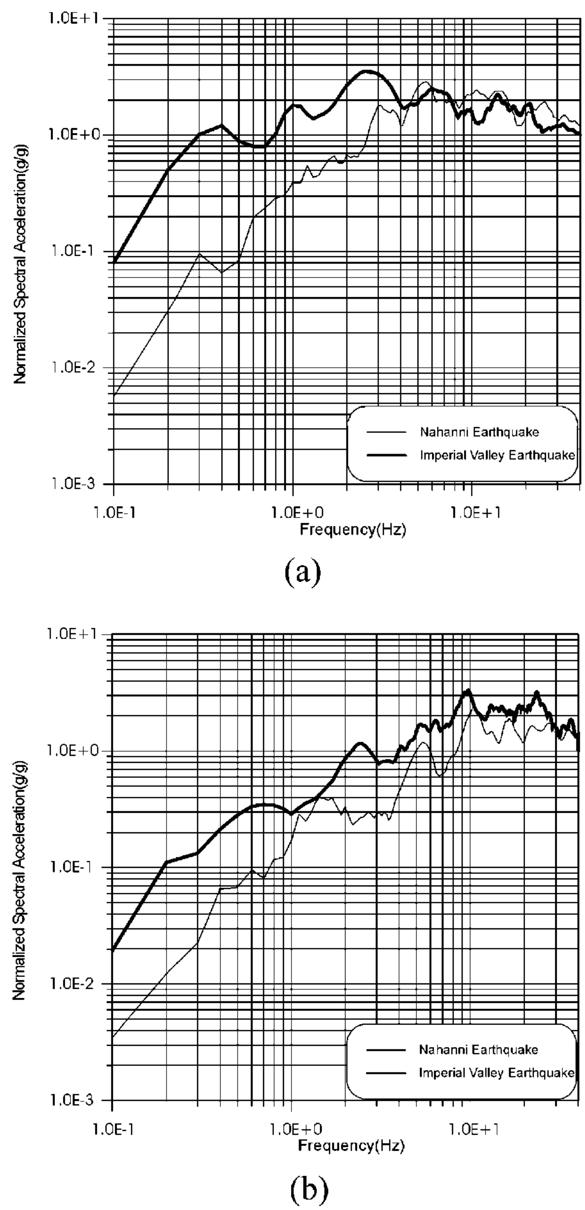

Fig. 9. Comparison of normalized ground acceleration response spectra of Nahanni and Imperial Valley earthquakes for 5% damping; (a) H1 component, (b) V component

used in model 2 to simulate the soft soil condition. The topographic and local soil characteristics of both Kyungju City and El Centro areas are similar.

The time histories and ground response spectra with 5 per cent damping, normalized to maximum acceleration, of both earthquakes are shown in Figures 8 and 9. The tail parts of the time histories longer than 20 s were cut off in the test. It is noted that the low-frequency content of the Imperial Valley earthquake is more distinct than that of the Nahanni event. Three components of each earthquake were input simultaneously during the tests. The vertical component was scaled to 2/3 of the horizontal. The PGA was increased from $0{\cdot}1g$ to $0{\cdot}6g$ in increments of $0{\cdot}1g$ for model 1 of rock condition, whereas the PGA was increased from $0{\cdot}05g$ to failure in increments of $0.05g$ for model 2 of soft soil condition. In a related but separate test, random white noise was input for measuring the natural frequency and damping ratio at elastic level.

4. TEST RESULTS

4.1. Natural frequency and damping ratio

The fundamental natural frequencies of model 1 measured in the elastic range for the white noise input with peak acceleration of $0{\cdot}025g$ were 3·32 Hz and 3·52 Hz in the longitudinal and transverse directions, respectively. Those of model 2 for the same input were 3·32 Hz and 4·29 Hz,

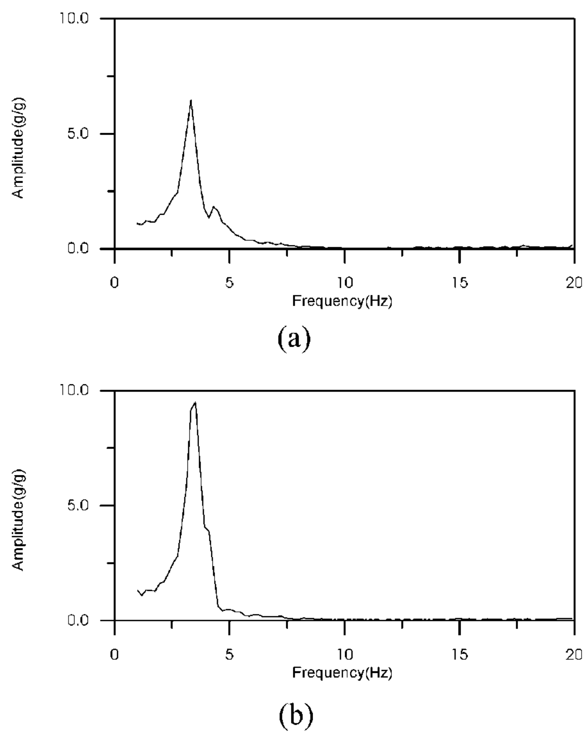

Fig. 10. Transfer function of the model 1 for random white noise; (a) longitudinal direction, (b) transverse direction

respectively. The difference of natural frequency in transverse direction was thought to be the difference in model fabrication and carpenter's skill. The transfer function of model 1 measured at column A3 for random white noise input is shown in Figure 10. Since the length scale is 1/4, the frequency of the model is twice that of the prototype.[7]

The modal damping ratio of the wooden house in the elastic range measured from Figure 10 is about 7 per cent in both directions. It is noted that an equivalent viscous damping ratio of the frame system measured from the cyclic load tests for large displacements[2] is 27 and 13 per cent in the longitudinal and transverse directions, respectively.

4.2. *Structural responses*

The acceleration and displacement responses of each model were measured for different PGA input levels. Peak responses of model 1 at the top of column A3 for the rock site condition are summarized in Table I. Acceleration responses were filtered using a low-pass Butterworth filter. It is noted that the acceleration response in the horizontal direction is reduced significantly compared with the input PGA as the input level is increased; however, the absolute value increases gradually as the PGA level of input increases. Acceleration and displacement responses in a longitudinal (x) direction are larger than the transverse (y) direction because of the difference in energy content of the motion. The vertical acceleration response is slightly increased compared with the input PGA. Model 1 was moderately damaged at PGA of $0{\cdot}6g$, and suffered a permanent displacement in longitudinal direction.

The maximum responses of the model 2 at the top of columns A3, C2, and D1 for soft soil condition are given in Table II. Acceleration responses were also low-pass filtered. The trends in acceleration and displacement response are almost the same as for model 1, but the model 2 collapsed in the longitudinal direction at a much lower PGA level of $0.25g$ (Figure 11). Maximum longitudinal and transverse displacements occurred at the D1 and A3 columns, respectively. Some torsional behaviour of the model was noted.

The actual PGA level of collapse or severe damage may be greater than indicated by this test program. Since the repetitive testing and scaling processes adopted no doubt induced cumulative damage in the models.

Table I. Maximum response of model 1 at the top of the A3 column for Nahanni earthquake

Input PGA level		$0{\cdot}1g$	$0{\cdot}2g$	$0{\cdot}3g$	$0{\cdot}4g$	$0{\cdot}5g$	$0{\cdot}6g$
Displacement response (mm)	X	1·19	2·85	3·91	6·24	7·83	9·84
	Y	1·08	3·28†	5·89†	4·69	6·21	7·40
	Z	—	—	—	—	—	—
Acceleration response (g)	X	0·067	0·086	0·111	0·056‡	0·168	0·172
	Y	0·052	0·071†	0·082†	0·063‡	0·087	0·153
	Z	0·093	0·173	0·251	0·024‡	0·379	0·398

*Acceleration responses were low-pass filtered at 50 Hz.
†Accelerations were input 150–170 per cent greater than specified level in all frequency bands.
‡Data measured are not reliable.

Table II. Maximum response of model 2 at the top of columns A3, C2, and D1 for Imperial Valley earthquake

Input PGA level	Model response at top of the column						
	Direction	Max. acceleration (g)*			Max. displacement (mm)		
		A3	C2	D1	A3	C2	D1
	X	0·038	0·043	0·052	4·28	4·20	5·13
0·05g	Y	0·036	0·029	0·035	2·33	1·59	0·80
	Z	0·041	0·045	0·040	—	—	—
	X	0·056	0·058	0·064	9·74	9·40	10·71
0·08g	Y	0·045	0·040	0·041	4·13	3·14	2·44
	Z	0·072	0·078	0·072	—	—	—
	X	0·065	0·062	0·067	14·29	13·29	14·96
0·10g	Y	0·047	0·053	0·049	4·97	4·29	2·46
	Z	0·090	0·083	0·082	—	—	—
0·15g	X	0·099	—	—	—	—	—
0·20g	X	0·146	—	—	—	—	—
0·25g			Collapse				

*Responses were low-pass filtered at 50 Hz.

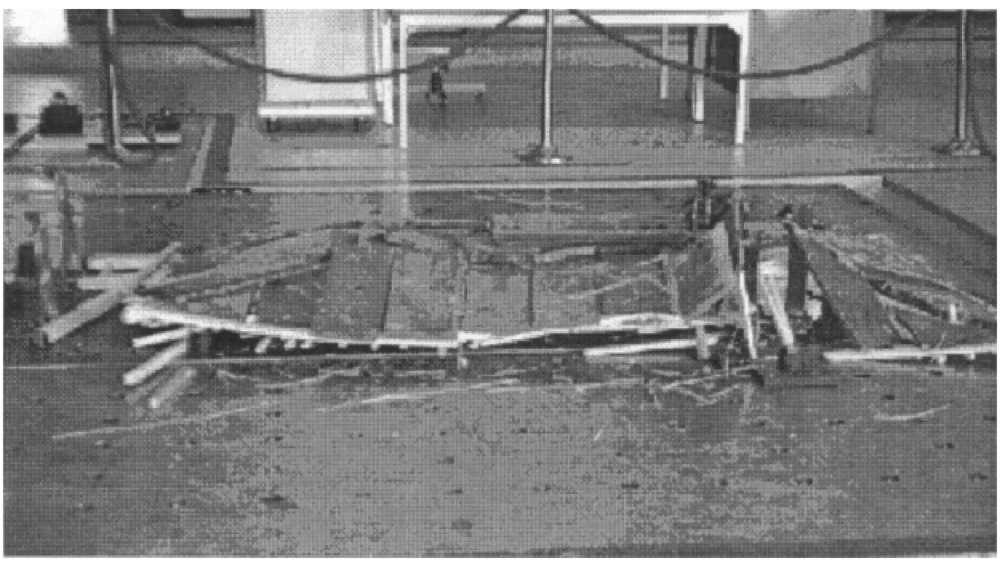

Fig. 11. Overview of collapsed model at PGA = 0·25g for Imperial Valley earthquake

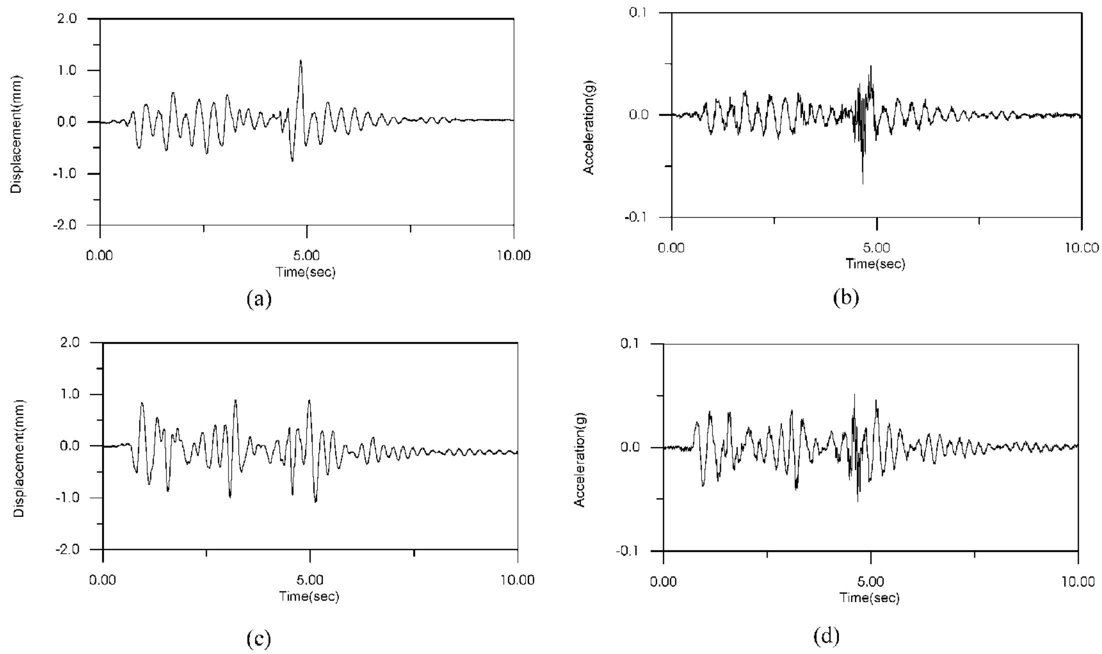

Fig. 12. Response time history of the model 1 at the A3 column for Nahanni earthquake, input PGA = $0{\cdot}1g$; (a) displacement in x-direction, (b) acceleration in x-direction, (c) displacement in y-direction; (d) acceleration in y-direction

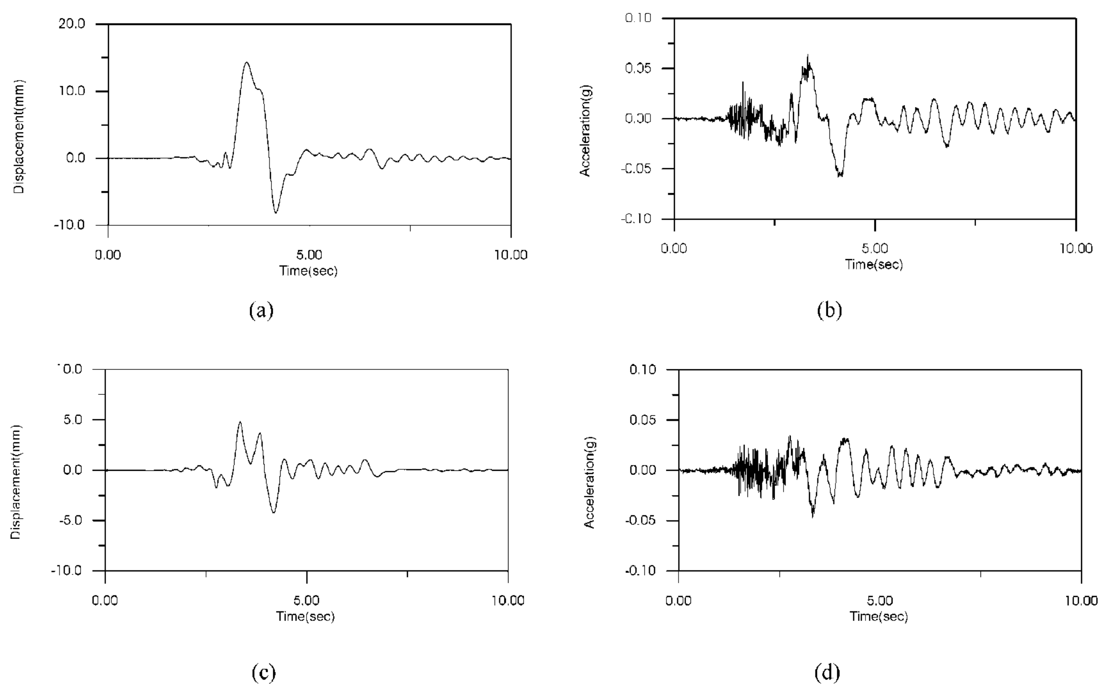

Fig. 13. Response time history of the model 2 at the column A3 for Imperial Valley earthquake, input PGA = $0{\cdot}1g$; (a) displacement in x-direction, (b) acceleration in x-direction, (c) displacement in y-direction; (d) acceleration in y-direction

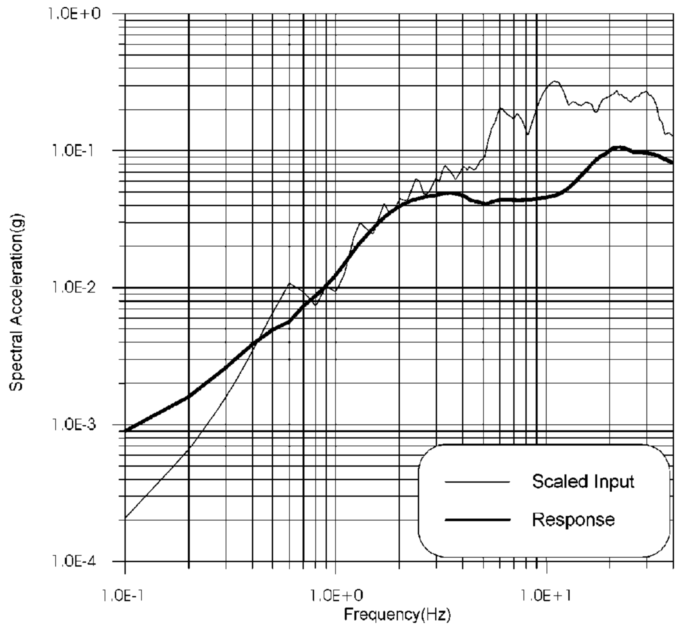

(a)

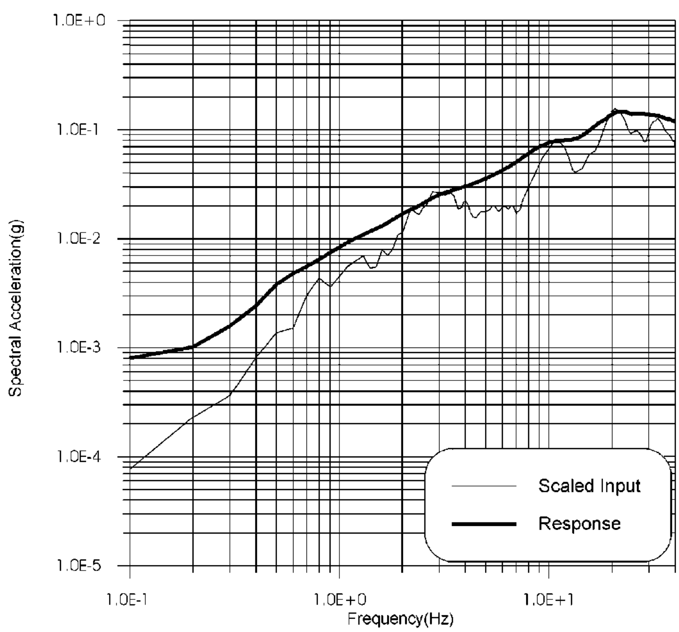

(b)

Fig. 14. Acceleration response spectra of the Model 1 for Nahanni earthquake at the column A3, PGA = $0{\cdot}1g$; 5% damping for input motion and V component, and 27% damping for H1 component; (a) H1 component, (b) V component

The fundamental frequency of the models measured by random test after $0.6g$ test for model 1 and $0{\cdot}1g$ test for model 2 is 3·32 Hz and 3·13 Hz in the longitudinal direction (x), respectively. There was no stiffness reduction in model 1. It was shown that the large experienced displacement induce the stiffness reduction in case of model 2. However, the stiffness reduction is not so large that the acceleration level of house collapsing may not be affected greatly by cumulative damage from repetitive testing.

The typical response time histories in the horizontal direction of each model measured at the top of column A3 for $0{\cdot}1g$ input acceleration are shown in Figures 12 and 13. It is noted that the acceleration and displacement time histories are similar in shape in model 1. Model 1 vibrates at its fundamental frequency in Figure 12, because it behaves mostly in the elastic range. Model 2 vibration is almost the same as the input in the beginning as shown in Figure 13, because low peaks with high-frequency components are contained in the front part of the input time history. However, it vibrates at its fundamental frequency after it experiences a large displacement.

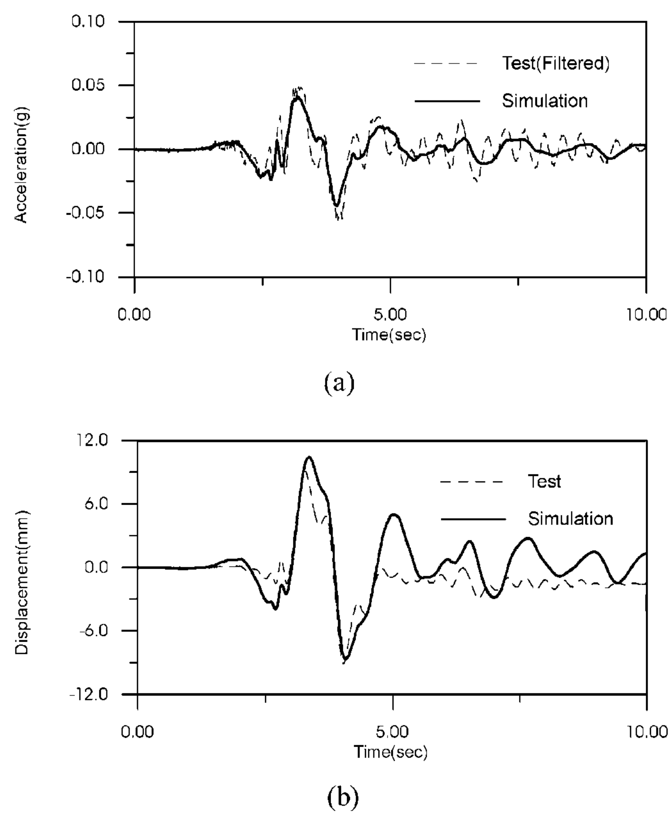

Fig. 15. Comparison of the results of test and simulation, Imperial Valley earthquake, input PGA $= 0{\cdot}08g$, x-direction; (a) acceleration response, (b) displacement response

Typical acceleration response spectra of the model 1 at the A3 column for PGA of 0.1g are shown in Figure 14. It can be seen that horizontal acceleration is reduced but the vertical acceleration is slightly increased.

5. NONLINEAR DYNAMIC ANALYSIS AND DISCUSSION

Non-linear dynamic analyses using the modified Double-Target model[2,8] were performed and compared with test results to verify its validity. Model parameters such as stiffness and damping ratio, which were obtained from full-scale frame tests, were used. Test models were idealized as single-degree-of-freedom lumped mass systems.

Figures 15 and 16 compare the acceleration and displacement responses of model 2 at the top of column A3. One horizontal component of motion with PGA of 0·08g was input in each direction. It is noted that both analytical and test results agree quite well in general. However, the analytical model yields a rather large maximum displacement and small acceleration responses.

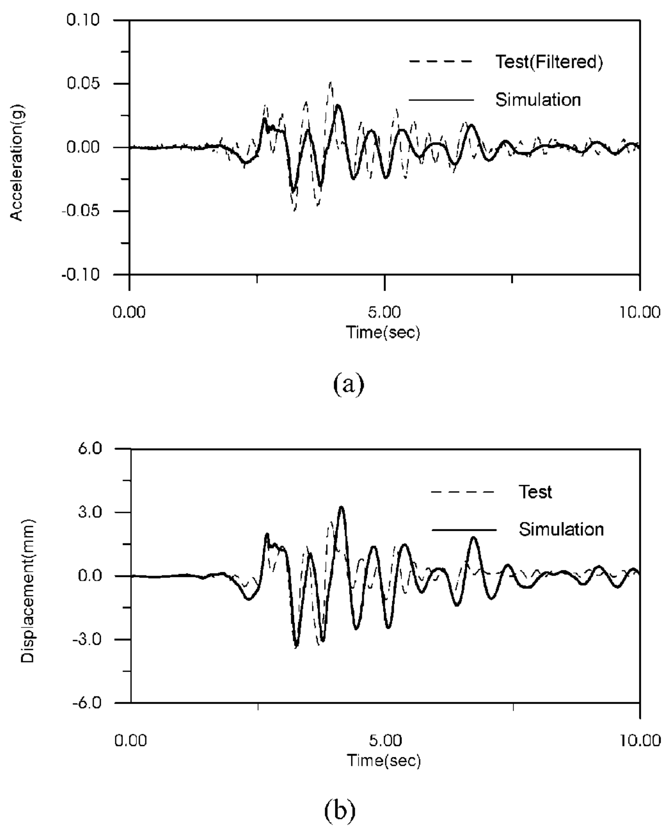

Fig. 16. Comparison of the results of test and simulation, Imperial Valley earthquake, input PGA = 0·08g, y-direction; (a) acceleration response, (b) displacement response

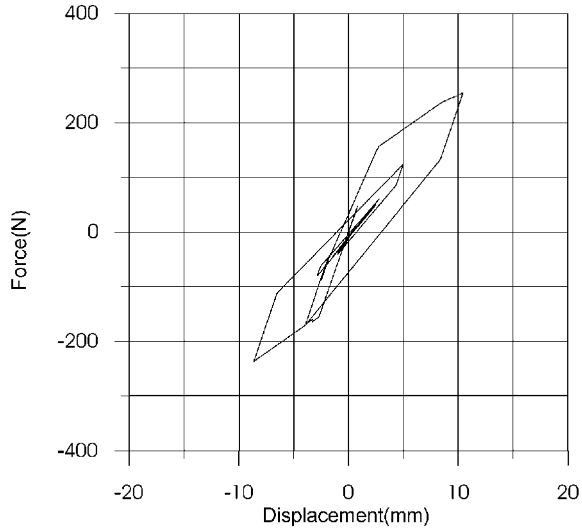

(a)

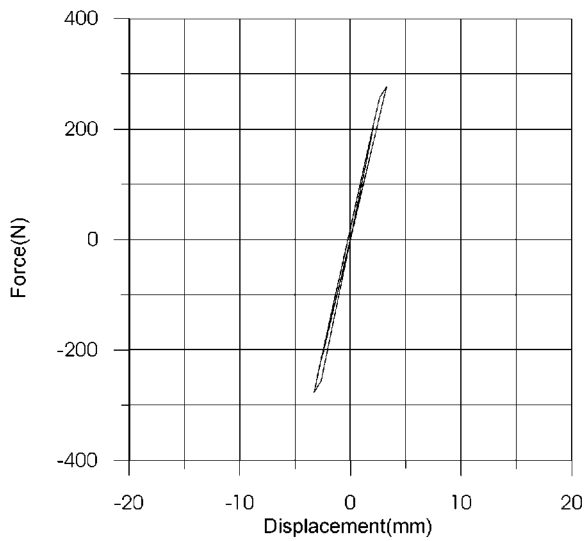

(b)

Fig. 17. Load–displacement curves, input PGA = 0·08g, modified Double-Target model; (a) x-direction, (b) y-direction

This phenomenon is remarkable in the y-direction and is judged that the stiffness of frames of the prototype house in the analytical model was estimated less in a transverse direction than actual values. In reality, both type 1 and type 2 frames were used in a transverse direction and these were represented by type 2 frames in the analytical model. The analytical results also show long

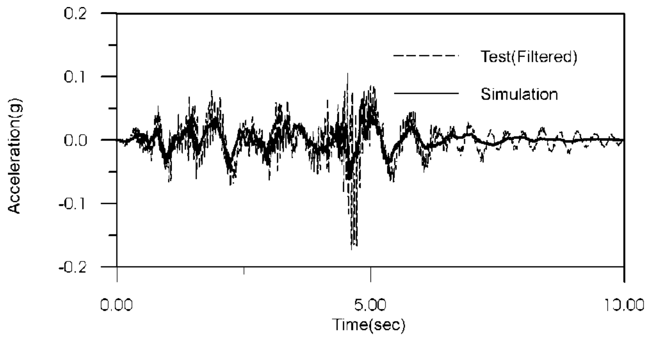

(a)

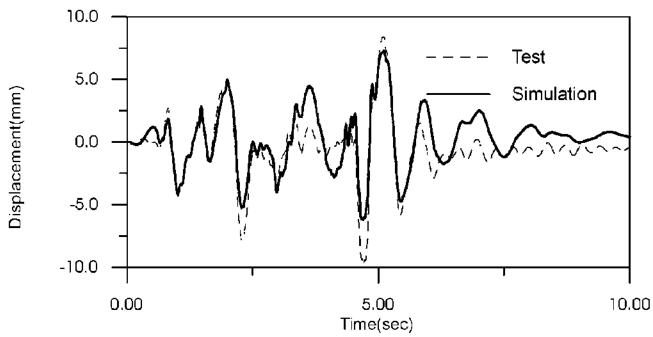

(b)

Fig. 18. Comparison of the results of test and simulation, Nahanni earthquake, input PGA = 0·6g, x-direction; (a) acceleration response, (b) displacement response

period responses after the model experiences maximum displacement. The maximum displacement of the model obtained from the analytical model in longitudinal direction is 10·4 mm which is 26·8 per cent larger than the test result of 8·2 mm. The hysteretic curves of the idealized frame are shown in Figure 17. Significant non-linear inelastic behaviour in longitudinal direction is noted.

The acceleration and displacement responses of the model 1 at the top of column A3 for input PGA of 0·6g are compared in Figures 18 and 19. The analytical results are for the horizontal component only, whereas, test results are for three components of motion input simultaneously. It can be noted that both results agree well and the structural behaviour in the horizontal direction is de-coupled. However, the analytical model shows smaller responses than the test results. In comparison with the displacement responses in longitudinal direction, the maximum displacement obtained from simulation is 6·2 mm, which is 37 per cent smaller than the test result of 9·8 mm. The secondary effect due to large displacement and gravity load combined with vertical component of motion, accumulation of repeated

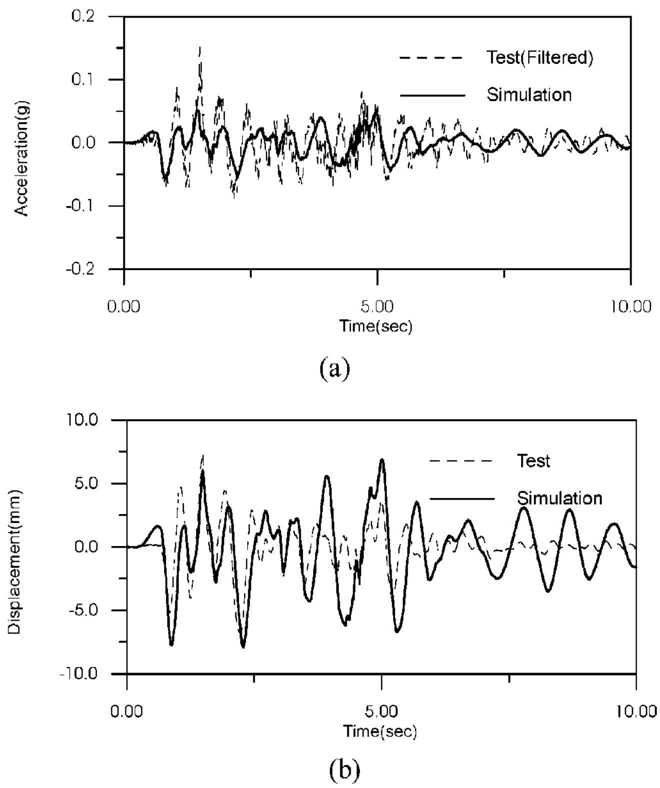

Fig. 19. Comparison of the results of test and simulation, Nahanni earthquake, input PGA = $0{\cdot}6g$, y-direction; (a) acceleration response, (b) displacement response

damages, etc. could be the sources of difference, which were not analysed in this study. Significant non-linear inelastic behaviours are also noted in the hysteretic curves of the idealized frame in Figure 20.

6. CONCLUSION

Shake table tests on the 1 : 4 scaled models of an ancient Korean commoner's house made of fresh pine lumber were performed. Tenon joints constituted wooden frames. Typical earthquake time histories recorded at soil and rock sites were used for input motion. The PGA level was increased step by step until the models experience severe damage or failure. The results of non-linear dynamic analyses based on the modified Double-Target model were compared with the test results. The following conclusions are derived from the study.

The fundamental natural frequency and modal damping ratio of the ancient wooden house in the elastic range are 1·66 Hz and 7 per cent, respectively. The traditional wooden house is very flexible and shows non-linear inelastic behaviour so that the horizontal acceleration responses are significantly reduced compared with the input. The wooden house is very weak in soil sites. The peak ground acceleration at the collapse of the house in soil site is

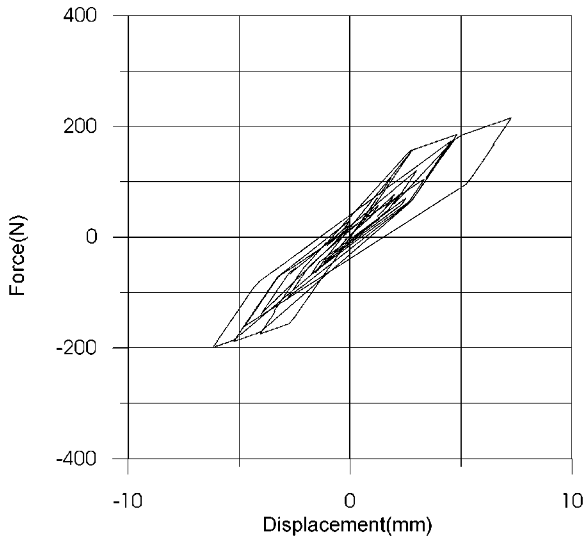

(a)

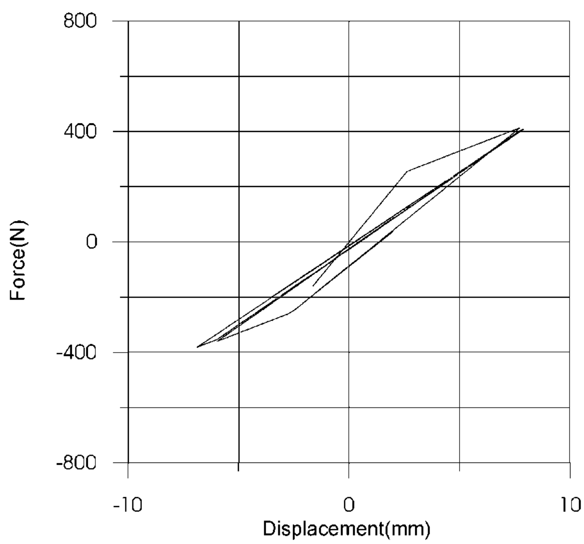

(b)

Fig. 20. Load–displacement curves, input PGA = $0{\cdot}6g$, modified Double-Target model; (a) x-direction, (b) y-direction

$0{\cdot}25g$, whereas the house in rock site is moderately damaged at $0{\cdot}6g$. The modified Double-Target model can appropriately simulate the non-linear inelastic behaviour of a wooden house with tenon joints.

REFERENCES

1. Applied Technology Council, *ATC-13: Earthquake Damage Evaluation Data for California,* National Science Foundation, 1985.

2. Jeong-Moon Seo, In-Kil Choi and Jong-Rim Lee, 'Static and cyclic behavior of wooden frames with tenon joints under lateral load', *ASCE J. Struct. Engng.* **125**(3)**,** 344–349 (1999).
3. Jeong-Moon Seo, In-Kil Choi and Jong-Rim Lee, 'A study on the structure and lateral loading capacity of wooden frame of ancient commoner's house', *J. Earthquake Engng. Soc. Korea*, **1**(2)**,** 31–37 (1997) (in Korean).
4. Jeong-Moon Seo, In-Kil Choi, and Jong-Rim Lee, 'Hysteretic characteristics of wooden frames of three-bay-straw-roof house under lateral cyclic load', *J. Earthquake Engng. Soc. Korea* **1**(3)**,** 21–27 (1997) (in Korean).
5. Jeong-Moon Seo, In-Kil Choi, and Jong-Rim Lee, 'A test on the aseismic capacity of a traditional three-bay-straw-roof house (I); Rock site condition'. *J. Earthquake Engng. Soc. Korea* **1**(4)**,** 11–20 (1997) (in Korean).
6. Jeong-Moon Seo, In-Kil Choi, and Jong-Rim Lee, 'A test on the aseismic capacity of a traditional three-bay-roof house (II); Soil site condition', *J. Earthquake Engng. Soc. Korea*, **1**(4)**,** 21–28 (1997) (in Korean).
7. R. S. Mills, H. Krawinkler and J. M. Gere, 'Model tests on earthquake simulators development and implementation of experimental procedures', The John A. Blume Earthquake Engineering Center, Department of Civil Engineering, Stanford University, 1979.
8. Y. Ohtori and K. Ishida. 'Effect of experienced shear strain dependency of high damping rubber bearing on earthquake response of isolation structure'. *J. Struct. Constr. Engng.*, Architectural Institute of Japan **472**, 75–84 (1995) (in Japanese).

